Stabilization of severe slugging based on a low-dimensional nonlinear model

E.Storkaas, S.Skogestad*

Department of Chemical Engineering

Norwegian University of Science and Technology, Trondheim, Norway

November 1, 2002

Abstract

Conventional models for multiphase flow are based on partial-differential equations. If these are to be used for conventional controller design and analysis, one would have to discretize the system into a large set of ODE's. Analysis and design are complicated due to the large state dimention.

We have developed a simpilfied nonlinear model with 3 states of gravity-induced slug flow that are suitable for control purposes. By fitting the model to data from the rigorous multiphase simulator OLGA, we show that we can get a good representation of the process with our simplified model.

A controllability analysis shows that the best measurement alternative for a stabilizing controller is upstream pressure. If this measurement is not available, a flow measurement at the downstream choke valve can be used to stabilize the system. In the latter case, closing the stabilizing loop will result in an (almost) integrating system. Higher level control loops may experience bandwidth limitations due to RHP zeros caused by the unstable poles in the inner loop.

A simple PI controller stabilizes the system with upstream pressure measurements. When a cascade control structure based on downstream flow measurements and valve reset is implemented, the bandwidth of the system is lowered significantly due to bandwidth limitations, but stable operation is achieved.

*email: skoge@chemeng.ntnu.no

1 Introduction

Offshore production of oil is moving towards more satellite wells and greater depths. The multiphase pipeline-riser systems needed to transport the oil to the production platform gives rise to an uneven multiphase flow regime known as slug flow. Gravity-induced slug flow occures as a result of a lowpoint connected to an inclining section of the pipe. The pressure drop in the pipeline and the interphase friction between the phases are in these cases not sufficient to transport the liquid uphill in a stationary fashion. The liquid will accumulate at the lowpoint, and a liquid slug will form.

The liquid slug that forms will block the flow of gas in the pipe, and grow until enough upsteam pressure has developed to overcome the weight of the liquid slug. These slugs can grow very large, and cause severe problems when they are delivered to the downstream production facility. The inlet separator will experience large level variation, resulting in poor separation and in some cases flooding. Load variations on the compressors may lead to unnecessary flaring. One or all of this problems may result in poor regularity. Another aspect is that the pressure variation caused by slug flow might lead to reduced well preformance.

Early solutions to the slug problem were based on stationary arguments and included increasing pressure drop over the topside production chokes, installation of expensive slug-catchers and injecting lift-gas into the riser to reduce slugging. Increasing the pressure drop over the upsteam choke efficiently eliminiates slugging, but it also increases the total pressure drop in the well-pipeline system, resulting in lower oil recovery. Stabilizing the flow at a lower pressure drop using active control has a great economic potential both in improved regularity and the possibility for increased recovery of oil.

There are currently several successful implementations of control systems that stabilizes the flow at a pressure drop that would result in slug flow in open-loop operation. The earliest experiments were made by Statoil in 1987 (Hedne and Linga, 1990). References to other implementations can be found in Henriot et al. (1999) and Havre et al. (2000). These controllers are primarily based on experiments and simulations using rigorous multiphase simulators like OLGA. Our earlier work (Storkaas et al., 2001) used a PDE-based model, resulting in high dimentional models. The need for a simpler model was evident. We have developed a simplified model that can be fitted to experimental data and used for more thorough analysis and controller design.

We will demonstrate that even simple linear controllability analysis based on the simplified model can provide invaluable information about the control problem. We will utilize this information for designing linear controllers that will stabilize the system.

2 Model

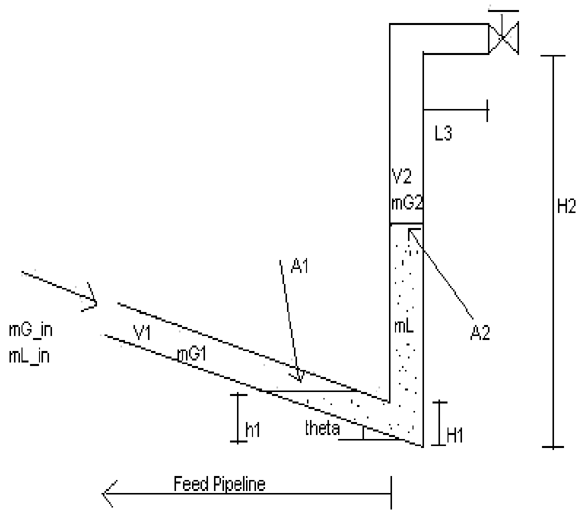

Figure 1: Illustration of system with feed pipeline, "lowpoint", riser and choke valve

2.1 Modelling principles

Based on our work on severe slugging it has become evident that we need a low-dimentional, simplified model in order to study the control implications of such a system. Nonlinear properties of the system can be important when it comes to breaking the limit cycle and bringing the system to its desired steady state operating point. These nonlinear characteristics are very hard to study with a PDE based model with 50 or more states (after discretizing in space).

We have made a model with 3 states, based on a system as depicted in figure 1. Our main assumptions are:

- Constant liquid velocity in "feed" pipeline (neglecting liquid level dynamics). This implies:
  - Constant upstream gas volume (volume variations due to liquid level at the lowpoint are neglectable)
  - Constant liquid feed directly into riser
- Only one liquid control volume (which includes part of the feed pipeline)
- Two gas control volumes, separated by the lowpoint, and connected through a pressure-flow relationship.
- Ideal gas law
- Stationary pressure balance between riser and feed section
- Simplified choke model for gas and liquid leaving the riser

2.2 Notation

The term riser is used for the part of the system from the lowest point to the valve.

Symbol	Description	Unit	Remarks
m_{Gi}	Mass of gas in volume i	Kg	State variable
m_L	Mass of liquid	Kg	State variable
V_{Gi}	Gas volume i	m^3	$V_{G1} = const$
V_L	Volume occupied by liquid	m^3	
V_{LR}	Volume of liquid in riser	m^3	
V_T	Total volume in riser	m^3	
P_i	Pressure in volume i	$\frac{N}{M^2}$	
ρ_{Gi}	Gas density in volume i	$\frac{kg}{m^3}$	
ρ_L	Liquid density	$\frac{kg}{m^3}$	Constant
$\bar{\rho}$	Average density in riser	$\frac{kg}{m^3}$	
ρ_T	Density upstreams valve	$\frac{kg}{m^3}$	
v_{G1}	Gas velocity at lowpoint	$\frac{m}{s}$	
$v_{mix,out}$	Liquid velocity through choke valve	$\frac{m}{s}$	
$\dot{m}_{G1}$	Internal gas mass flowrate	$\frac{Kg}{s}$	
$\dot{m}_{G,out}$	Gas mass flowrate through choke valve	$\frac{Kg}{s}$	
$\dot{m}_{L,out}$	Liquid mass flowrate through choke valve	$\frac{Kg}{s}$	
α_L	Average liquid fraction in riser, volume basis	-	
α_{LT}	Liquid fraction upstreams valve, volume basis	-	
α_L^m	Liquid fraction upstreams valve, mass basis	-	
h_1	Liquid level upstreams the dip	m	
H_1	Critical liquid level	m	Constant
H_2	Height of riser	m	Constant
r	Radius of pipe	m	Constant
A_1	Area in horizontal plane, V_1	m^2	Constant
A_2	Cross section area, V_2	m^2	Constant
$\hat{A}$	Gas flow area at lowpoint	m^2	
L_3	Length of horizontal top section	m	Constant
θ	Feed pipe inclination	rad	Constant
R	Gas constant	$8314 \frac{J}{K \cdot Kmol}$	Constant
g	Spesific gravity	$9.81 \frac{m}{s^2}$	Constant
T	System temperature	K	Constant
M_G	Molecular weight of gas	$\frac{Kg}{Kmol}$	Constant
$\dot{m}_{G,in}$	Mass rate of gas into system	$\frac{Kg}{s}$	Disturbance
$\dot{m}_{L,in}$	Mass rate of liquid into system	$\frac{Kg}{s}$	Disturbance
P_0	Pressure after choke valve	$\frac{N}{M^2}$	Disturbance
z	Valve position	-	Input
K_1	Choke valve constant	-	Tuning parameter
K_2	Gas flow constant	-	Tuning parameter
K_3	Friction parameter	-	Tuning parameter
n	w^n in the friction expression	-	Tuning parameter

2.3 Equations

Internal Equations

$$P_1 = \frac{m_{G1} RT}{V_{G1} M_G} \tag{1}$$

$$\rho_{G1} = \frac{m_{G1}}{V_{G1}} \tag{2}$$

$$V_L = \frac{m_L}{\rho_L} \tag{3}$$

$$h_1 A_1 + V_{LR} = V_L \tag{4}$$

$$V_T = A_2 \left(H_2 + L_3 \right) \tag{5}$$

$$V_{G2} = V_T - V_{LR} \tag{6}$$

$$\rho_{G2} = \frac{m_{G2}}{V_{G2}} \tag{7}$$

$$\alpha_L = \frac{V_{LR}}{V_T} \tag{8}$$

$$P_2 = \frac{m_{G2} RT}{V_{G2} M_G} \tag{9}$$

$$\bar{\rho} = \frac{m_{G2} + V_{LR} \rho_L}{V_T} \tag{10}$$

$$\bar{\rho} g \left(H2 + H3 \right) - \rho_L g h_1 = P_1 - P_2 \tag{11}$$

$$\begin{aligned} \alpha_{LT} = {} & \left(V_{LR} > H_2 A_2 \right) \frac{V_{LR} - A_2 H_2}{A_3 H_3} \\ & + \frac{w^n}{1 + w^n} \left(\alpha_L - \left(V_{LR} > H_2 A_2 \right) \frac{V_{LR} - A_2 H_2}{A_3 H_3} \right), w = \frac{K_3 \rho_{G1} v_{G1}^2}{\rho_L - \rho_{G1}} \end{aligned} \tag{12}$$

$$\rho_T = \alpha_{LT} \rho_L + \left(1 - \alpha_{LT} \right) \rho_{G2} \tag{13}$$

$$\alpha_L^m = \frac{\alpha_{LT} \rho_L}{\alpha_{LT} \rho_L + \left(1 - \alpha_{LT} \right) \rho_{G2}} \tag{14}$$

Transport Equations

$$v_{G1} = \left(h_1 < H_1 \right) K_2 \frac{H_1 - h_1}{H_1} \sqrt{\frac{P_1 - P_2 - \rho_L g \alpha_L H_2}{\rho_{G1}}} \tag{15}$$

$$\dot{m}_{G1} = v_{G1} \rho_{G1} \hat{A} \tag{16}$$

$$m_{mix,out} = K_1 z \sqrt{\rho_T \left(P_2 - P_0 \right)} \tag{17}$$

$$\dot{m}_{G,out} = \left(1 - \alpha_L^m \right) m_{mix,out} \tag{18}$$

$$\dot{m}_{L,out} = \alpha_L^m m_{mix,out} \tag{19}$$

Geometric Equations

$$H_1 = \frac{2r}{cos\left(\theta\right)}$$

$$A_1 = \frac{A_2}{sin\left(\theta\right)}$$

$$\phi = \left(\left(H1 - h1\right) cos\left(\theta\right) < r\right) \left(\pi - acos\left(1 - \frac{\left(H1 - h1\right) cos\left(\theta\right)}{r}\right)\right) +$$

$$\left(\left(H1 - h1\right) cos\left(\theta\right) > r\right) \left(acos\left(\frac{\left(H1 - h1\right) cos\left(\theta\right)}{r} - 1\right)\right)$$

$$\hat{A} = r^2 \left(\pi - \phi - cos\left(\pi - \phi\right) sin\left(\pi - \phi\right)\right) \tag{20}$$

Conservation Equations

$$\frac{d}{dt} m_L = \dot{m}_{L,in} - \dot{m}_{L,out} \tag{21}$$

$$\frac{d}{dt} m_{G1} = \dot{m}_{G,in} - \dot{m}_{G1} \tag{22}$$

$$\frac{d}{dt} m_{G2} = \dot{m}_{G1} - \dot{m}_{G,out} \tag{23}$$

2.4 Comments on the equations

Most of the equations are straight forward: ideal gas law, mass balances, volume balances for liquid (constant density), density definitions and volume/mass fraction computations. The stationary pressure balance (eq.11) assumes that we can neglect dynamic effects, acceleration and wall friction. A simplified valve equation (eq.17) is used for the choke, with the assumption of preserved mass fraction through the choke. Instead of impulse balances in the pipe, a pressure-flow relationship for gas (eq.15) and an entrainment equation for the liquid (eq.12) is used.

With its current states, the model must be solved as a differential-algebraic (DAE) system, but with a state transformation, it is possible to transform the system into an ODE system. The state transformation si shown in appendix 1.

2.4.1 Relationship between gas flow and pressure drop

For the gas phase, neglecting the acceleration terms, the pressure difference $\Delta P = P_1 - P_2$ is the sum of the frictional pressure drop and the static pressure drop.

$$\Delta P = \Delta P_f + \rho_L g h \tag{24}$$

For turbulent flow

$$\Delta P_f = \sum_i c_i \rho_i \frac{v_i^2}{2} \tag{25}$$

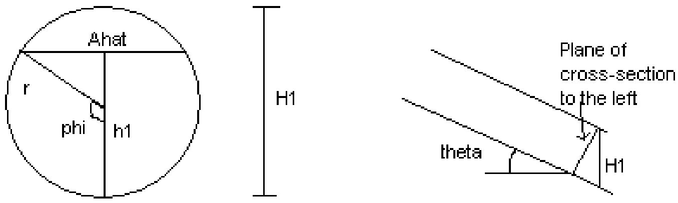

Figure 2: Geometric basis for calculating $\hat{A}$

where ΔP_i is the individual frictional pressure losses. Focusing on the lowpoint and assuming that the pressure drop here is purely frictional, we get

$$\Delta P = (P_2 - P_1 - \rho_L g \alpha_L H_2) = c\rho_{G1}\frac{v_{G1}^2}{2} \tag{26}$$

Clearly, the factor c depends on the relative "opening" $\frac{H_1-h_1}{H_1}$, and assuming an inverse quadratic dependence gives eq. 15. The corresponding massflow is given by eq. 16, where $\hat{A}$ is the gas flow area at the lowpoint which is calculated as illustrated in figure 2. $\hat{A}$ is calculated on a cross-section of the declining pipe (hence the $cos\,(\theta)$ in the calculation of ϕ). Note that combining equations 15 and 16 with $f\,(h_1) = \left(\frac{H_1-h_1}{H_1}\hat{A}\right)$, yields a 'valve equation'.

$$\dot{m}_{G1} = K_2 f\,(h_1)\sqrt{\rho_{G1}\,(P_1 - P_2)} \tag{27}$$

where the functional dependency of $\left(\frac{H_1-h1}{H_1}\right)$ is approximatly quadratic.

2.4.2 Entrainment equation

Given the assumptions abowe, the only thing that is missing is an equation to determine the velocity of the liquid. Instead of using a slip relation similar to the one used in *drift flux* modelling, we found that it was better (and easier) to use an equation relating the fraction of liquid in the top to the internal gas velocity. This is equivalent to an entrainment equation.

The two extreme cases are no entrainment (liquid behaves as if in a tank) for zero gas velocity and no slip ($\alpha_{LT} = \alpha_L$) for high gas velocities. The entrainment in slug flow is somewhat similar to flooding in destillation columns. The flooding velocity in destillation columns (which is equal to the terminal velocity for a falling liquid drop) is given by

$$v_f = k\sqrt{\frac{\rho_L - \rho_G}{\rho_G}} \tag{28}$$

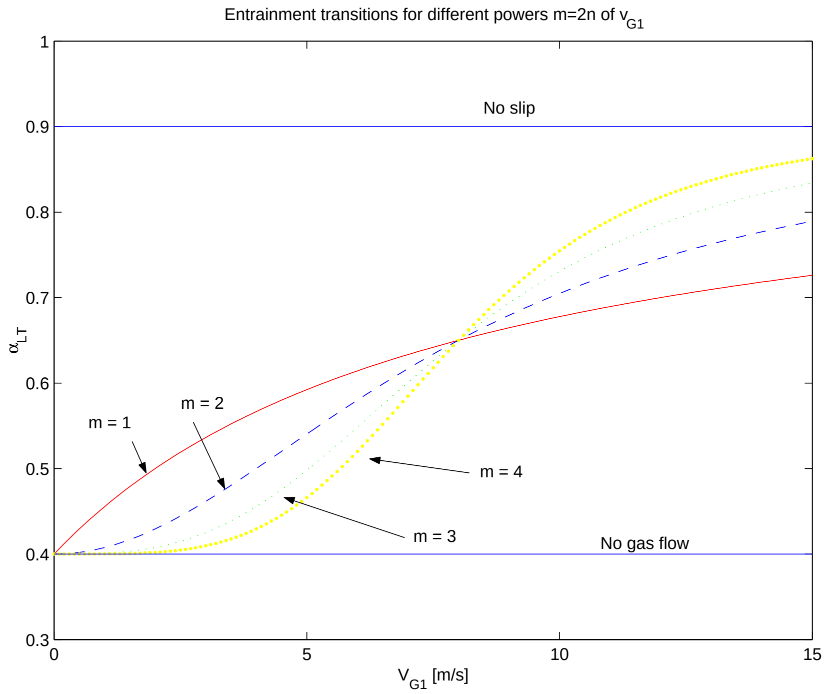

Figure 3: Entrainment transition for different powers of v_{G1}

This expression only gives a yes/no answer to whether it is flooding or not. The transition between the two extremes should preferably be continous, and one way of doing that is to assume that the transition depends on $\frac{v_{G1}}{v_f}$ and use the form

$$\alpha_{LT} = \alpha_{LT,Noflow} + \frac{w^n}{1+w^n}(\alpha_L - \alpha_{LT,Noflow})$$

where

$$w = k\frac{v_{G1}^2}{v_f^2} = \frac{K_3 \rho_{G1} v_{G1}^2}{\rho_L - \rho_{G1}}$$

The transition for different orders of velocity is shown in figure 3. The exponent n is a tuning parameter used to achieve the effect of a lower limit and a quicker transition described above.

Note that we use the velocity at the lowpoint (v_{G1}) to obtain the entrainment of liquid through the riser. This is because the impulse of the gas at the lowpoint initiates the entrainment by affecting the velocity of the incompressible liquid. By assuming that the average gas impulse responsible for the entrainment of liquid through the riser is linearly dependent on the impulse of gas through the lowpoint, our use of v_{G1} in the entrainment equation is justified.

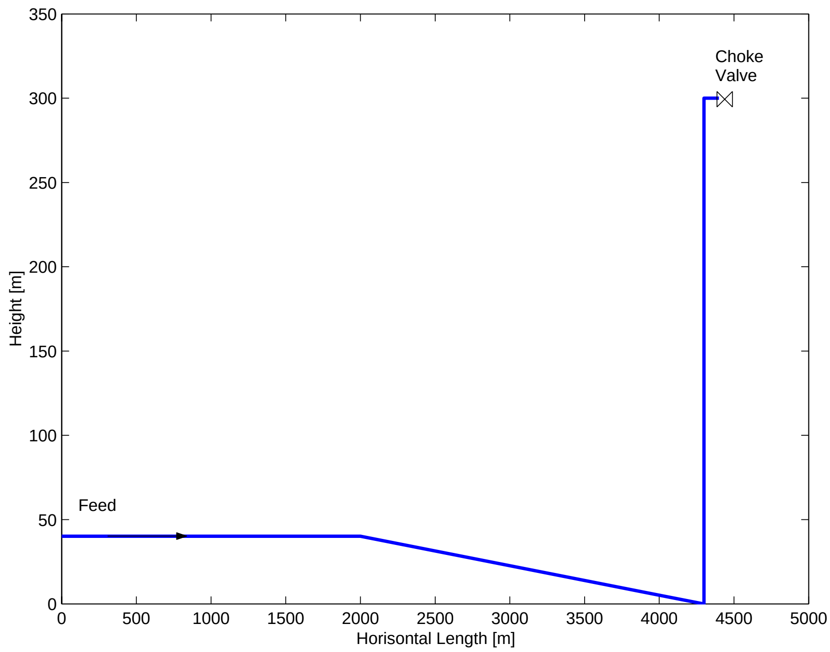

Figure 4: Geometry for the test case

V_{G1}	ρ_L	r	H_2	L_1	T	M_G	P_0
$12m^3$	$750\frac{kg}{m^3}$	$0.12m$	$300m$	$100m$	$308K$	$35\frac{kg}{kmol}$	$50bar$

Table 1: Case Data

3 Case Study

In order to verify the model, we will compare it to results from OLGA, which is the standard industrial tool for multiphase flow simulations. For simplicity, we will use the test case for severe slugging in OLGA. The only change we made to the case was to use a slightly smaller choke valve in order to get better control authority.

The case geomery is given in figure 4 and other case data is given in table 1.

3.1 Initialization

At steady state, the model has 27 variables, including 4 parameters (n, K_1, K_2 and K_3) to be determined, and 23 equations. The stationary value of h_1 must lie in the intervall $0 \leq h_1 < H_1$, and for the tuning of the model, iterating on a fixed h_1 is a good idea to ensure consistency. We focus on the Hopf point found from the OLGA simulations, and from that we can get data for P_1 and P_2. If we also fix n, we can find the values of K_1, K_2 and K_3. By

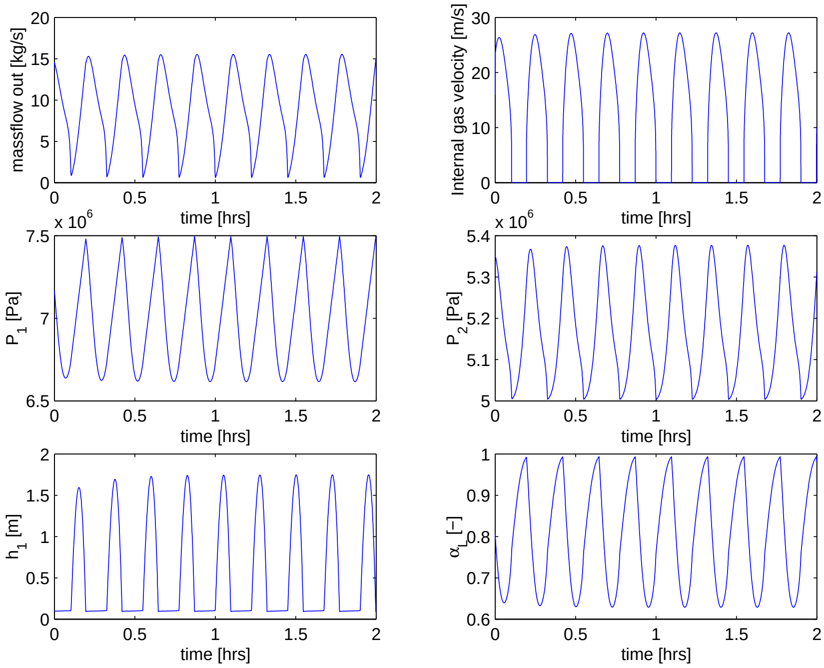

Figure 5: Simulation results with z=0.2

iterating on the fixed values and checking the linear (eg. stability) properties, the bifurcation diagram and nonlinear (open loop behaviour) properties of the resulting model, suitable tuning constants can be found.

Tuning the model for n=2.25 with z=0.13 yields

h_1	P_1	P_2	K_1	K_2	K_3
$0.94H_1$	$71.7 \cdot 10^5$	$53.5 \cdot 10^5$	0.005	12.86	0.051

3.2 Simulations

With the data given above and a valve opening of 0.2, the results for a two hour simulation is given in figure 5.
The bifurcation diagram for the system is given in figure 6.
The unstable poles of the system moves further into the RHP as the valve opening increases, as can be seen if figures 7 and 8.

The model is tuned to achive the best possible fit to the stationary data obtained from OLGA. As can be seen from the bifurcation diagrams (fig. 6), the fit for the stationary data is excellent, while the fit for the amplitude is satisfactory, especially in the low- to medium valve opening range. Deviations for larger valve openings are not surprising, since a very simple valve model is used, and the model is tuned to optimize the fit for low- to medium valve openings.

The main deviation is in the frequency of the limit cycle. The simplified

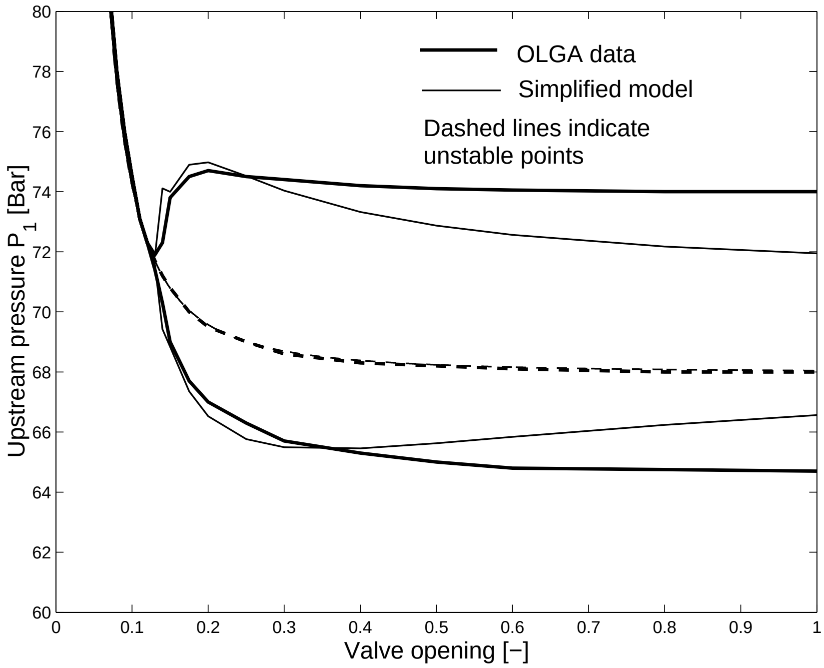

Figure 6: Comparison of bifurcation diagrams

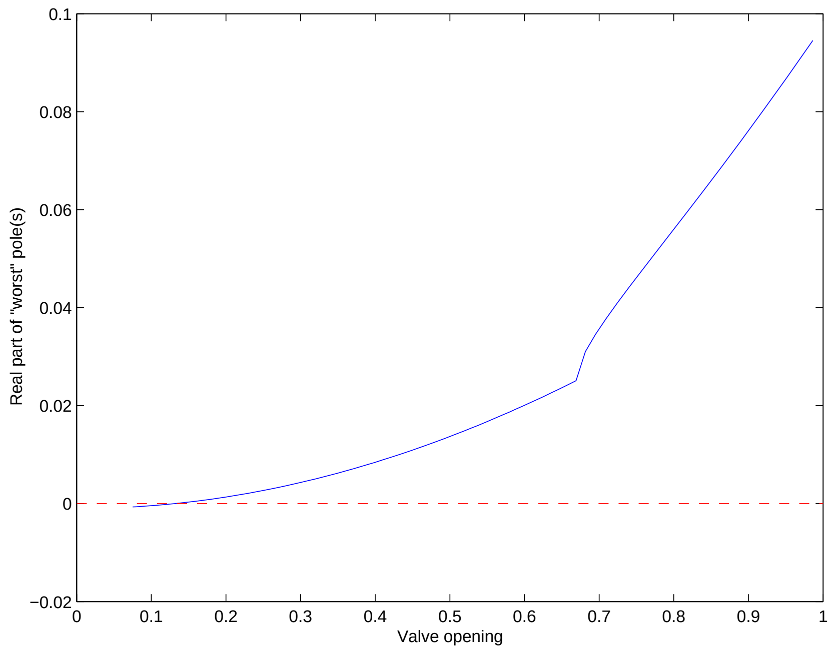

Figure 7: Real part of the "worst" pole as function of valve position

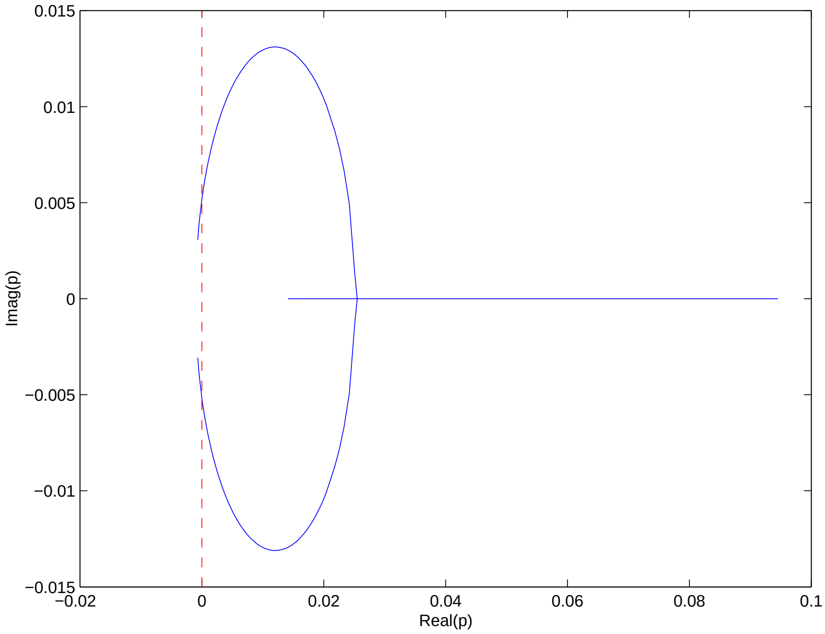

Figure 8: Root locus diagram for the simplified model

Symbol	Physical Entity
P_1	Upstream pressure
P_2	Downstream pressure (before choke valve)
ρ_{mix}	Mixture density through choke
Q	Total volumetric flow through choke
W	Total massflow through choke

Table 2: Measurement alternatives

model predicts a frequency that is higher than that of the OLGA model. This is probably due to neglected liquid level dynamics in the pipe upstream the riser. To get the same amplitude, we use a relatively low volume upstream (V_{G1}) in the simplified model. In reality, this volume is not constant, and the volume variations will decrease the frequency.

4 Controllability analysis

We will in this section assume that the choke valve is our only actuator option. We will consider several options for measurements, presented in table 2.

For the operating point with z=0.25, the poles for the system are -6.2095 and $0.0028 \pm 0.0090i$. The zeros for the different measurements are given in table 3. For a SIMO control configuration with combinations of two or more measurements, the system has no zeros.

P_1	P_2	ρ_{mix}	q	W
-0.0034	0.0131	-0.0004	-4.6276	-7.7528
-	3.4828	0.0048	-0.0032	-0.0004
-	-	-	-0.0004	0

Table 3: Zeros for different measurement alternatives

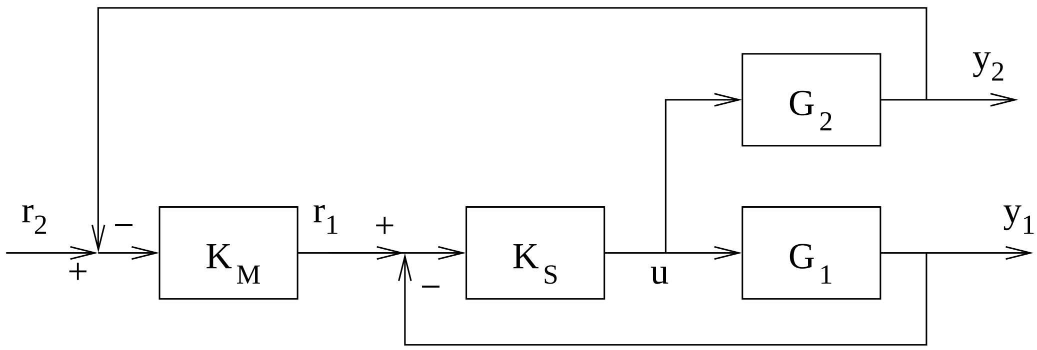

Figure 9: Block diagram for a cascade control system

Obviously, the best choice of measurement would be the upstream pressure P_1. However, this measurement can in many cases be either unreliable or unavaliable, and other measurements should also be considered. Of the alternatives in table 3, both P_2 and ρ_L have RHP-zeros close to the unstable poles, and are not suitable as measurements for a stabilizing controller due to the bandwidth limitations imposed. Volume flow Q and mass flow W are better alternatives, but both have zeros close to or at the imaginary axis. Stabilizing the system with one of these measurements would result in an (almost) integrating closed loop system, but using a cascade configuration could solve that problem.

The block diagram for the cascade control configuration is given in figure 9. Here G_1 is the transfer function from the input z to the flow measurements, and G_2 is the transfer function from input u to the output to the master controller K_M. K_S is the stabilizing controller in the inner loop.

The input sensitivity function from input disturbance to input for the inner loop is given by $S_I = (1 + G_1 K_S)^{-1}$. To ensure internal stability, the unstable poles in G_1 cannot be cancelled by K_S, hence S_I must have RHP-zeros in the same location as the unstable poles in G_1. The process transfer function for the outer loop will be $G_M = G_2 S_I K_S$. If G_2 contains the same instability as G_1, the RHP-zeros in S_I will be cancelled. If not, they will limit the bandwidth for the master controller in the cascade. In the latter case, e.g. with input resetting in the outer loop ($G_2 = 1$), the faster the instability, the higher the limit in bandwidth. In other words, a difficult stabilization task in the inner loop will allow for faster control in the outer loop and vice versa.

In our case, the most natural alternatives are either input reset or downstream pressure control in the outer loop. With input reset, the unstable poles of G_1 will occure as RHP-zeros in G_M. With pressure control in the outer loop, the same unstable poles exists in G_1 and G_2, and the RHP-zeros in S_I will be cancelled by G_2. However, the bandwidth will still be limited by G_2's own RHP-zeros.

5 Control configuration evaluation

For the simulations in this section, the process is started up in open loop, as can be seen from the initial ocillatory behaviour. The controller is turned on at t=0.5 hrs, with a set point corresponding to an operating point with $P_1 = 70bar$ (valve opening 0.175). At t=1.5 hrs, the set point is changed to $P_1 = 69bar$ (valve opening 0.25). At t=2.5 hrs, the set point is changed back to its initial value.

5.1 Upstream pressure control

If an upstream pressure measurement is available, a simple pressure controller (PI) will stabilize the system. In figure 10 a PI controller with gain K=0.5 bar^{-1} and interal time τ_i = 500s is stabilizing the system from an initial severe slugging behaviour to an operating point with z= 0.25 and P_1= 69 bar.

5.2 Cascade control with downstream measurements

Upstream pressure measurements are in many cases not even installed. In those cases were they are, they can be unreliable or for other reasons poorly suited for control, and it would be beneficial not to have to rely on those. Controlling the mass or volume flow through the choke valve results in an integrating system. However, by using a cascade control system with the valve position in the outer loop, this can be dealt with. The mass and volume flow can be estimated by measuring the pressure drop over the choke and the mixture density.

In figure 11 the system is stabilized with the above mentioned cascasde controller. The tuning parameters for the inner loop are K=10 s/m^3, $\tau_i = 40s$ and for the outer loop K=0.001 m^3/s and $\tau_i = 750s$. The operating point is the same as with the pressure controller.

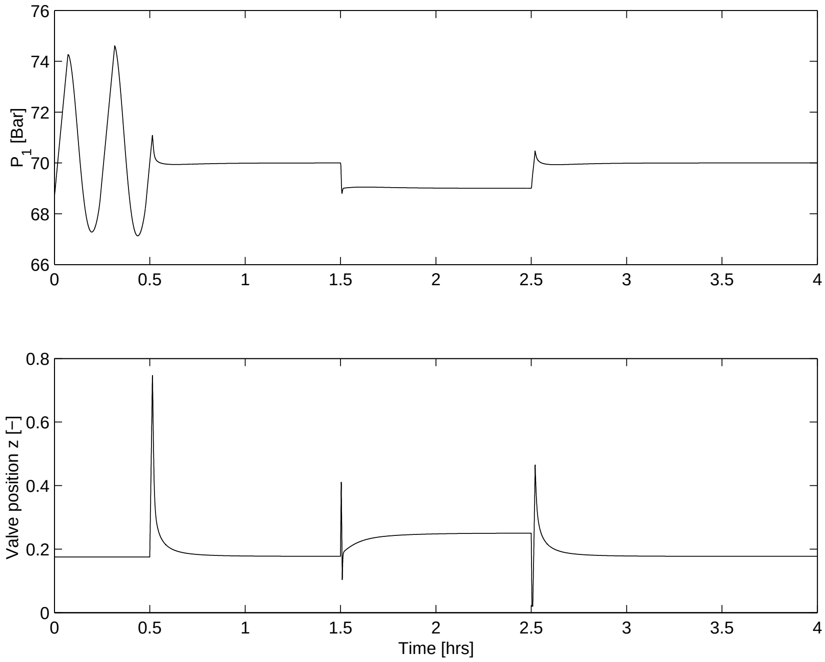

Figure 10: Stabilization with a SISO pressure controller

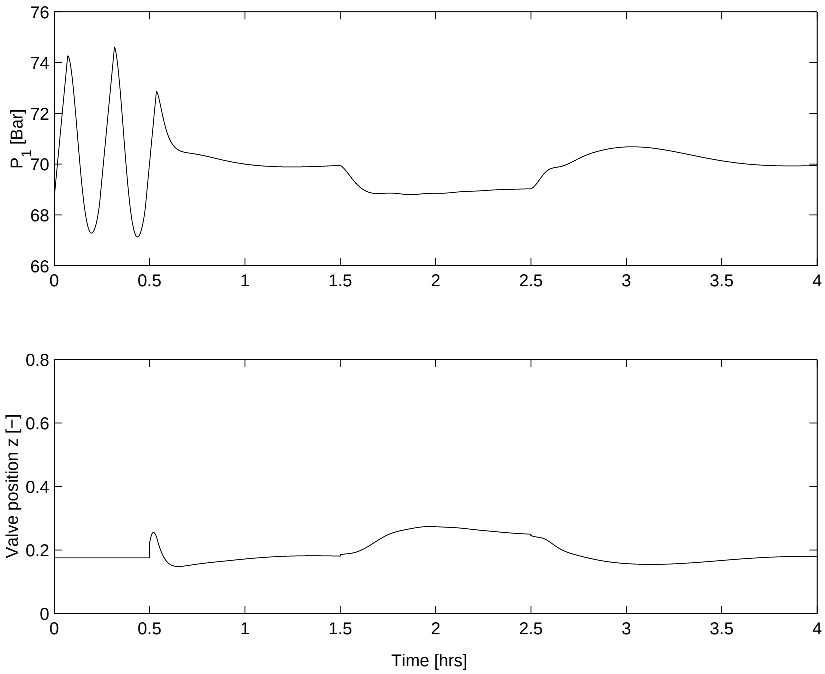

Figure 11: Stabilization with a upstream cascade controller

6 Conclusions

We have developed a simpilfied nonlinear model of gravity-induced slug flow that is suitable for control purposes. By fitting the model to data from the rigorous multiphase simulator OLGA, we have shown that we can get a good representation of the process with our simplified model.

A controllability analysis shows that the best measurement alternative for a stabilizing controller is upstream pressure. If this measurement isn't available, a flow measurement at the downstream choke valve can be used to stabilize the system. In the latter case, closing the stabilizing loop will result in an (almost) integrating system. Higher level control loops may experience bandwidth limitations due to RHP zeros caused by the unstable poles in the inner loop.

A simple PI controller stabilizes the system with upstream pressure measurements. When a cascade control structure based on downstream flow measurements and valve reset is implemented, the bandwidth of the system is lowered significantly due to bandwidth limitations, but stable operation is achieved.

References

Havre, K., Stornes, K. and Stray, H. (2000), 'Taming slug flow in pipelines', *ABB review* **4**, 55–63.

Hedne, P. and Linga, H. (1990), 'Supression of terrein slugging with automatic and manual riser choking', *Advances in Gas-Liquid Flows* pp. 453–469.

Henriot, V., Courbot, A., Heintze, E. and Moyeux, L. (1999), 'Simulation of process to control severe slugging: Application to the dunbar pipeline', SPE Annual Conferance and Exibiton in Huston,Texas. SPE 56461.

Storkaas, E., Skogestad, S. and Alstad, V. (2001), 'Stabilization of desired flow regimes in pipelines', AIChE Annual meeting, Reno, Nevada. Paper 287d.

Appendix 1

State transformation

To simplify the notation, we will scale and rename the states m_L, m_{G1} and m_{G2} to $x_1 = \frac{m_L}{V_T \rho_L}$, $x_2 = \frac{m_{G1}}{V_{G1}\rho^\star_{G1}}$ and $x_3 = \frac{m_{G1}}{V_T \rho^\star_{G2}}$. The quantities marked with an asterix are reference values for the given variable. When x is used without subscript, it is taken to mean all the states when used as an argument or the state vector when used in an expression. When $(\cdot)$ is used as an argument, it is an abbreviation to simplify the notation and should be taken to represent the appropriate arguments for the given expression.

With the current states, the model is a DAE system. The height h_1 will be used as the algebraic state, denoted γ. Entries that are not states and that are not given with an argument are constant system parameters.

With these changes of notation, we can simplify the model to:

$$\dot{x}_1 = \frac{\dot{m}_{L,in}}{V_T \rho_L} - \frac{\alpha_{LT}(\cdot)\left(1 - x_1 + \frac{A_1}{V_T}\gamma\right)}{\alpha_{LT}(\cdot)\rho_L\left(V_T - V_T x_1 + A_1\gamma\right) + V_T\rho^\star_{G2}\left(1-\alpha_{LT}(\cdot)\right)x_3}\Psi(\cdot)\, z \tag{29}$$

$$\dot{x}_2 = \frac{\dot{m}_{G,in}}{V_{G1}\rho^\star_{G1}} - \frac{\hat{A}(\gamma)\, v_{G1}(\cdot)\, x_2}{V_{G1}} \tag{30}$$

$$\dot{x}_3 = \frac{\rho^\star_{G1}\hat{A}(\gamma)\, v_{G1}(\cdot)\, x_2}{V_T\rho^\star_{G2}} - \frac{\left(1-\alpha_{LT}(\cdot)\right)x_3}{\alpha_{LT}(\cdot)\rho_L\left(V_T - V_T x_1 + A_1\gamma\right) + V_T\rho^\star_{G2}\left(1-\alpha_{LT}(\cdot)\right)x_3}\Psi(\cdot)\, z \tag{31}$$

$$\left(\rho^\star_{G2}x_3 + \rho_L x_1 - \frac{\rho_L A_1}{V_T}\gamma\right) g\left(H2 + H3\right) - \rho_L g\gamma = \frac{RT}{M_G}\left(\rho^\star_{G1}x_2 - \frac{V_T\rho^\star_{G2}x_3}{\left(V_T - V_T x_1 + A_1\gamma\right)}\right) \tag{32}$$

v_{G1}, Ψ and α_{LT} used above is given below. $\hat{A}(\gamma)$ is given by equation 20.

$$v_{G1}(x,\gamma) = (\gamma < H_1)\, K_2 \frac{H_1 - \gamma}{H_1}\sqrt{\frac{\frac{RT}{M_G}\left(\rho^\star_{G1}x_2 - \frac{V_T\rho^\star_{G2}x_3}{(V_T - V_T x_1 + A_1\gamma)}\right) - \rho_L g H_2\left(x_1 - \frac{A_1}{V_T}\gamma\right)}{\rho^\star_{G1}x_2}}$$

$$\Psi\left(x,\gamma,\alpha_{LT}(\cdot)\right) = \frac{m_{mix,out}}{z} = K_1\sqrt{\left(\alpha_{LT}(\cdot)\rho_L + \frac{V_T\rho^\star_{G2}\left(1-\alpha_{LT}(\cdot)\right)x_3}{V_T - V_T x_1 + A_1\gamma}\right)\left(\frac{V_T\rho^\star_{G2}RTx_3}{\left(V_T - V_T x_1 + A_1\gamma\right)M_G} - P_0\right)}$$

$$\alpha_{LT}\left(x,\gamma,v_{G1}(\cdot),\tilde{\alpha}_{LT}(\cdot)\right) = \tilde{\alpha}_{LT}(\cdot) + \frac{\left(K_3\rho^\star_{G1}x_2 v^2_{G1}(\cdot)\right)^n}{\left(\rho_L - \rho^\star_{G1}x_2\right)^n + \left(K_3\rho^\star_{G1}x_2 v^2_{G1}(\cdot)\right)^n}\left(x_1 - \frac{A_1}{V_T}\gamma - \tilde{\alpha}_{LT}(\cdot)\right)$$

$$\tilde{\alpha}_{LT}(x,\gamma) = \left(V_T x_1 - A_1\gamma > H_2 A_2\right)\frac{V_T x_1 - A_1\gamma - A_2 H_2}{A_3 H_3}$$

Solving algebraic equation for x_2

$$x_2 = \Phi(x_1,x_3,\gamma) = \frac{M_G g\left(H2 + H3\right)}{RT\rho^\star_{G1}}\left(\rho^\star_{G2}x_3 + \rho_L x_1 - \frac{\rho_L A_1}{V_T}\gamma\right) - \frac{\rho_L M_G g}{RT\rho^\star_{G1}}\gamma + \frac{V_T\rho^\star_{G2}x_3}{\rho^\star_{G1}\left(V_T - V_T x_1 + A_1\gamma\right)}$$

Differentiating $\Phi\left(x_1, x_3, \gamma\right)$:

$$\frac{\partial\Phi}{\partial x_1} = \frac{M_G g \rho_L \left(H2 + H3\right)}{RT\rho^\star_{G1}} - \frac{V_T^2 \rho^\star_{G2} x_3}{\rho^\star_{G1}\left(V_T - V_T x_1 + A_1\gamma\right)^2}$$

$$\frac{\partial\Phi}{\partial x_3} = \frac{M_G g \rho^\star_{G2} \left(H2 + H3\right)}{RT\rho^\star_{G1}} + \frac{V_T \rho^\star_{G2}}{\rho^\star_{G1}\left(V_T - V_T x_1 + A_1\gamma\right)}$$

$$\frac{\partial\Phi}{\partial\gamma} = -\frac{\rho_L M_G g}{RT\rho^\star_{G1}}\left(1 + \frac{A_1\left(H2 + H3\right)}{V_T}\right) + \frac{V_T A_1 \rho^\star_{G2} x_3}{\rho^\star_{G1}\left(V_T - V_T x_1 + A_1\gamma\right)^2}$$

The state transformation is:

$$\dot{\gamma} = \frac{\dot{x}_2 - \frac{\partial\Phi}{\partial x_1}\dot{x}_1 - \frac{\partial\Phi}{\partial x_3}\dot{x}_3}{\frac{\partial\Phi}{\partial\gamma}}$$